

A Seven Element S-Band Coupled Oscillator Controlled Agile Beam Phased Array

R. J. Pogorzelski, R. P. Scaramastra, J. Huang, R. J. Beckon, S. M. Petree, and C. Chavez
Jet Propulsion Laboratory
California Institute of Technology
Pasadena, CA 91109

Abstract - This paper describes the design, fabrication, and testing of a seven element S-band phased array in which the beam is steered by means of a coupled oscillator technique. Seven MMIC-based voltage controlled oscillators were coupled via microstrip transmission lines in such a manner that they mutually injection locked and thus oscillated as an ensemble. The output of each oscillator was connected to a microstrip patch array element and the seven elements were disposed in a line on a Duroid substrate. The resulting antenna was characterized in benchtop tests revealing the relative phase behavior of the oscillators and in range tests producing far field pattern cuts. Patterns showing beams steered to several angles were obtained by applying appropriate tuning voltages to the end oscillators of the array.

I. BACKGROUND

Some years ago it was suggested that an array of coupled oscillators can be used to control the phase distribution across the aperture of an array antenna in such a manner as to effect steering of the beam without the use of phase shifters.[1] The behavior of such arrays of oscillators has been described in detail using a coupled set of non-linear differential equations.[2][3] These equations are derived by first describing the behavior of an individual oscillator with injection locking in the manner of Adler [4] and then allowing the injection signals to be provided by the neighboring oscillators in the array. More recently, an alternative description was developed by Pogorzelski, Maccarini, and York [5] in which the phase distribution across the array is represented by a continuous function governed by a partial differential equation of diffusion type. This formalism provides considerable insight concerning the relationship between the phase distribution and the tuning of the oscillators.

One result of the above theoretical treatments is detailed understanding of the beam steering scheme proposed by York and demonstrated in four element X-band arrays by Liao and York [1][2] . Their approach made use of the mutual coupling between the radiating elements of the array to achieve mutual locking of the oscillators. Thus, the element spacing was constrained by the necessary coupling strength. In another experiment, the coupling was accomplished by connecting the radiating elements by microstrip lines.[6] This also rendered the coupling dependent on the element disposition. In the approach described here, the coupling is achieved through microstrip

transmission lines between the oscillator resonators. The oscillator outputs are isolated from the resonators by buffer amplifiers intrinsic to the MMICs which were used. Thus, the element spacing is independent of the coupling and can be chosen for optimum performance of the radiating aperture. The theory provides the relationship between coupling phase (the phase shift through the coupling lines) and the ensemble frequency and locking range, relationships which were observed experimentally during the development of the present seven element array. Moreover, the theoretical results were shown to accurately predict the beam steering behavior of this array.

In this paper, we describe the fabrication of the array of voltage controlled oscillators, the experimental determination of the behavior of this array, and comparison of the experimentally observed behavior with theoretical predictions. We further discuss the design of the microstrip patch radiating aperture and the characterization of the resonant S-band elements. Finally, we describe the experimental measurement of the antenna patterns under various scan conditions.

II. THE VOLTAGE CONTROLLED OSCILLATORS (VCOs)

A commercial MMIC VCO suitable for operation at a nominal 2.5 GHz was selected¹ and a number of preliminary characterizations were performed to ascertain its suitability for the present application. The typical board layout used is shown in Figure 1. In anticipation of later array testing, a three oscillator board based on this layout was fabricated. Full wavelength lines were used for coupling the oscillators. This choice was made for compatibility with the parallel resonance determining the free running frequency of the oscillators.[3] However, the end oscillators were fitted with half wavelength lines to provide a one wavelength round trip path through which the end oscillators inject themselves resulting in the desired Neumann boundary condition.[5] This three oscillator design is shown in Figure 2 with an enlarged view of the center oscillator shown in Figure 3.

First, we tested the acquisition and tracking performance of a single oscillator. This was done by adding a coaxial connector at the end of a half wavelength line connected to one of the end oscillators. This allowed both the termination of the micro-strip line and the injection of a test signal. The injected signal was set to -16 then -6 dBmW and the ranges measured. A representative set of data is as follows. The lock/no-lock condition was determined by observing a spectrum analyzer trace of the output. Lock was determined by the suppression of intermodulation products. (The reason for a narrower bandwidth on the (-) side of the oscillator frequency with a higher level injected signal was not established.)

Signal Level	Acquisition Bandwidth	Tracking Bandwidth
--------------	-----------------------	--------------------

¹ We gratefully acknowledge the assistance of Professor R. A. York and Mr. P. F. Maccarini of the University of California, Santa Barbara in selecting the Pacific Monolithics MMIC for the experiment and designing the initial board layout.

	-MHz	+MHz	-MHz	+MHz
-16 dBmW	4.4	2.9	5.4	5.4
-6 dBmW	3.1	9.5	4.2	21.6

Following the single oscillator tests, the three oscillator linear array was tested. Surprisingly, this design was found to produce a 180 degree phase relationship between adjacent oscillators. This discovery led to an intensive effort aimed at resolving this unexpected result.

The three oscillator development provided a wealth of information about the coupled oscillators. The tuning function (dF/dV) of the individual oscillators from 2 to 3 GHz was determined by individual tests. It was assumed that with three similar tuning functions the oscillators could all be set to the same frequency and would lock (synchronize) when inter-connected. Initially, however, this however did not happen.

When the oscillators were interconnected there was a dramatic change in their tuning functions. The individual oscillators would no longer tune to the lower frequencies (which were available with no inter-connection). The tuning curves above approximately 2.6 GHz retain the same logarithmic characteristic as with no inter-connection but below 2.6 GHz the tuning curves become straight lines and the oscillators ceased to function below about 2.45 GHz. It appears that at 2.6 GHz a boundary exists for which the oscillator has different oscillatory modes on either side. Attempts to tune to this break point results in the oscillator jumping between two frequencies in a random fashion (motorboating). This was greatly reduced by means of bypass capacitors on the power supply traces and a better grounding arrangement for the MMIC.

III. FABRICATION AND BENCH TESTING OF AN ARRAY

At this point a seven oscillator linear array was fabricated using all of the features added to the three element array to improve its performance. This seven element array is shown in Figure 4 with an enlargement of the center oscillator shown in Figure 5. A partial schematic is illustrated in Figure 6 which includes an end oscillator and the oscillator adjacent to it. The rest of the circuit continues in like manner to the far end.

The theoretical treatment is based on the assumption that the Q of the coupling circuit is much lower than that of the oscillators. To assure that this is the case in our implementation, we terminated the 100 Ohm coupling lines in their characteristic impedance using 100 Ohm chip resistors as shown in Figure 6. This reduced reflections from the ends of the line so that energy storage on the line in the form of standing wave was minimized. Minimum energy storage implies minimal Q.

The layout of the oscillators was modified somewhat from the previous design. The inter-connecting (coupling) lines were meandered in a U shape such that they could easily

be made to be half or full wavelength or anything in between by moving the shorting bar along the U shaped portion.

The new layout also included a printed common ground interconnect trace beneath the MMIC with more through connections to the underside ground plane. This additional trace improved on the single point ground performance. Figure 7 illustrates a representative portion of the seven element array.

Some features include:

- The addition of coaxial connectors so that each of the oscillators could either be monitored or influenced by external injection.
- An increased component land area at the power supply pins so that 1 micro-Farad capacitors could be permanently added to each of the oscillator Vcc pins.
- The addition of a common tuning voltage bus so that only a single precision tuning supply was needed for test. Voltage tuning of the individual oscillators was accomplished by 10 turn potentiometers connecting each oscillator to the bus.

The seven oscillator linear array exhibited the same type tuning characteristics as the previous single oscillator and triple oscillator array circuits. The uncoupled oscillators, tested one at a time (no coupling), have a logarithmic tuning curve as illustrated in Figure 8. The frequency spread from maximum to minimum for all seven oscillators is a nominal 4.5 %. The entire group of seven transfer functions are plotted so that the spread may easily be observed.

Coupling the oscillators and tuning one at a time yields the same 2.6 GHz breakpoint as exhibited by the other previously built oscillators. Again, as before with the previous oscillators and arrays, the tuning curve is logarithmic above 2.6 GHz, straight below 2.6 GHz, and discontinues below approximately 2.45 GHz. The curves end because the oscillators cease to function below this lower frequency. The tuning curves for the seven coupled oscillators are illustrated in Figure 9.

Locking the array proved to be difficult. There is a narrow frequency range where locking is attainable. The locking range only exists in the straight (linear) portion of the tuning curve below 2.6 GHz. Locking was not possible above the 2.6 GHz breakpoint. When locked, the adjacent oscillators naturally fell into a 180 degree phase relationship. As mentioned above, this relationship was not expected and thus needed to be understood.

Investigation proceeded as follows: The actual electrical length of the inter-connecting 100 Ohm coupling line is 360 degrees (one wavelength). The phase shift of the oscillator tuning circuit adds some additional electrical length to the coupling circuits. It was conjectured that the additional coupling circuit phase shift might be involved in the 180

degree output relationship. Experiments were devised that would shorten the coupling line length. Figure 7 shows the line length adjustment scheme that was used. Shortening the line lengths by approximately $\frac{1}{4}$ wave allows the adjacent oscillators to lock in-phase. Locking is still only possible on the linear portion of the tuning curves but the relationship between adjacent oscillators at rest is now at the desired 0 degrees. Two theoretically predicted behaviors were observed and thus confirmed during this investigation. First, when the coupling lines are an odd multiple of a quarter wavelength in effective length, the locking range of the array is reduced to zero and no locking is possible. Second, when the coupling lines are an even multiple of a quarter wavelength in effective length, the ensemble frequency is equal to the tuning frequency of the individual oscillators whereas it differs from this value for other line lengths. This difference is maximized at odd multiples of a quarter wavelength.

Further experiments with the locking range for the array yielded results that were not entirely consistent with theoretical predictions. Instead of the maximum theoretical differential of ± 90 degrees between adjacent oscillators only ± 60 degrees was actually obtained. This was accomplished by either of two methods.

The first method involved injecting a phase stable signal to both end oscillators in the array with a phase changing line stretcher in series with one of the paths. The end oscillators being locked to the injected signal could be pulled in phase so as to cause the desired phase distribution across the array; that is, Stephan's scheme. [7]

The second method involved adjusting the tuning bias upward in voltage (and frequency) on one end oscillator and downward in voltage (and frequency) on the other end oscillator thus maintaining a constant average tuning frequency. The oscillators, being locked to their neighbors, do not actually change oscillation frequency. The result is that the array oscillator output signals remain at the same frequency but their differential phase is controlled by the tuning. It is believed that the inability to achieve the full 90 degree phase difference between adjacent oscillators was due to the limited tuning range available. That is, before 90 degrees was reached, one or more oscillator outputs decreased in amplitude to a level at which they no longer participate in the interaction.

IV. DESIGN AND FABRICATION OF THE RADIATING APERTURE

Each oscillator in the array provides an output RF signal properly phased with respect to the others. To radiate this signal, one must provide each oscillator with a properly designed radiating antenna element. Each element must be properly impedance-matched to the oscillator and must radiate the RF energy with a wide enough beamwidth to achieve wide-angle beam scanning capability. The overall array antenna beam will then be a result of the spatial power combining which takes place in the radiating aperture. A microstrip patch was selected as the radiator because of its low profile and small weight,

as well as its capacity to be conformally mounted onto a curved surface. This choice also provides negligible mutual coupling between the elements, a property which was confirmed by the agreement between the measured array pattern and that predicted theoretically neglecting mutual coupling. In addition, all array elements can be fabricated on a single slab of substrate material with a single chemical etching process, which can significantly lower the production time and cost.

A. The Microstrip Patch Element.

The configuration of a single microstrip patch element is shown in Figure 10, where a square metallic patch is constructed, by a conventional chemical etching process, on a thin dielectric substrate with a conducting ground plane situated beneath it. The square patch, which was designed to resonate at 2.50 GHz, has a dimension of 3.63 cm. It is designed by using the “Ensemble” computer software which employs an integral equation technique (Method of Moments). To have a comfortable bandwidth for the radiator, the dielectric substrate was designed to have a thickness of 0.16 cm with a relative dielectric constant of 2.5. This dielectric substrate is made of the Rogers Duroid™ teflon impregnated fiber-glass material which can survive extreme temperature variations of more than $\pm 100^\circ \text{C}$. The square patch is excited at its 50-ohm input-impedance location, which is 1.27 cm from the patch’s edge, by an SMA coax probe.

The calculated radiation patterns of the single-patch element in the two principal planes (E-plane and H-plane) are given in Figure 11 where relatively wide beamwidths are demonstrated. In the same figure, the calculated input impedance match, in terms of return loss, is also given. It shows that the antenna resonates at 2.505 GHz and has a 2:1 VSWR (-10 dB return loss) bandwidth of about 35 MHz (1.4%).

B. The Seven-element Microstrip Patch Array.

A seven element array achieves sufficiently narrow beamwidth to demonstrate the beam scanning with adequate beam resolution. The layout of this seven element array is sketched in Figure 12 and photographs of the actual fabricated array, top and bottom views, are shown in Figure 13. All seven elements are identical with detailed element design given in Figure 10. The seven elements are spaced uniformly with half free-space wavelength spacing of 6.0 cm at 2.50 GHz. They are fabricated by etching on a rectangular substrate panel of 51 cm x 15 cm. The elements are arrayed in the H-plane. In other words, the array, as it is shown in Figure 7, is vertically polarized. Calculated 0° -scanned and the 10° -scanned beams are shown in Figure 12.

The measured input return losses of all seven patch elements are very much the same, and a typical measured return-loss-versus-frequency plot is given in Figure 14. A resonant

frequency of 2.503 GHz and a bandwidth of 33 MHz were measured and found to be very close to the calculated values in Figure 11. The radiation pattern of the seven element array, measured with a conventional seven-way power divider, is shown in Figure 15. By using the conventional power divider, the radiation performance of the array can be independently assessed without including the effect of the oscillator circuits. Two patterns are shown, one with the antenna physically rotated 180 degrees about the boresight with respect to the other. Comparison of these indicates that the discrepancy between the actual and calculated ideal patterns in the first two sidelobes is not due to range artifact while that in the third sidelobe probably is in part a range effect. The measured array pattern, given in Figure 15 for the 0°-scanned case, is indeed a good one and is very similar to that calculated in Figure 12. This indicates that the 7-element microstrip array developed here is adequate for the oscillator array demonstration.

V. RANGE TESTING OF THE ARRAY ANTENNA

Having established that the seven element oscillator array could be mutually injection locked and could provide linear phase distributions suitable for beam steering and controllable by detuning the end oscillators, a matched set of seven cables was fabricated with which to connect the outputs of each of the seven oscillators to a corresponding microstrip patch element in the radiating aperture. In preparation for the measurement, each of the oscillators was tuned to 2.522 GHz measured with a spectrum analyzer (HP-8562A) and the voltage necessary to do this was recorded. However, it was found that the amplitudes of the oscillator outputs were not equal. In fact they varied over a range of approximately plus or minus 3.5 dB. Therefore, attenuators (pads) were inserted in each of the lines to equalize the amplitudes while maintaining equal phase change in each line. Having done this, the end oscillators were detuned by an amount necessary to create phase progressions corresponding to steering angles of 6.38, 9.59, and 12.84 degrees (phase differences between the end oscillators of 120, 180, and 240 degrees) and the necessary tuning voltages recorded. Then, the array was placed on the measurement range and patterns were measured using each of the above four tuning voltage configurations.

In anticipation of the need for a reference signal to which to lock the range receiver, provision was made to injection lock the center oscillator of the array to a master oscillator (HP-8648C) which would provide the necessary locking signal to the receiver. Thus, the oscillator array and the receiver were locked to the same signal during the measurement. However, it was found that the injection line to the center oscillator tank circuit, loaded the circuit thus changing its free running frequency to approximately 2.55 GHz. Nevertheless, when the injection signal was applied, the oscillator of course oscillated at the desired 2.523 GHz. According to the theory, the effect of this is a phase shift between the external injection signal and the output of the center oscillator but no effect is anticipated regarding the relative phase of the center oscillator and the others in the array. The anticipated phase shift with respect to the injection signal is of no

consequence in the measurement because the system only depends on the coherence of the reference signal and not on its absolute phase.

A uniform set of 10 dB pads was installed, one at the back of each of the patch elements in the radiating aperture to eliminate the effects of the mismatch due to operation off resonance, and a set of measurements was taken. This mismatch is evident in the return loss of approximately -7 dB at 2.53 GHz shown in Figure 14.

The antenna on the range positioner with master oscillator and power supplies is shown in Figure 16. The corresponding results are shown in Figures 17-20 in which the ensemble frequency and injection frequencies were 2.522 GHz. The chart associated with each graph shows the free running frequency to which each oscillator was tuned and the voltage required to tune it. Also shown is the relative output power level and relative phase of each oscillator under lock conditions. These levels, read from the spectrum analyzer, and phases, measured with a network analyzer (HP-8410A), were used to computationally predict the pattern shown in long dashes for each scan angle.

As a final check, the array was tuned for 6.38 degrees of scan and the pattern was measured at roll angles of 0 and 180 degrees. Then the 180 degree pattern was reversed and plotted over the 0 degree pattern. This effectively compares measurements with the anechoic chamber rotated 180 degrees about the boresight. The comparison is a measure of the degree to which chamber artifacts have affected the measurement accuracy. In the absence of chamber asymmetries, the two patterns would overlay perfectly. The results of this test are shown in Figure 21. It is noted that chamber asymmetries are below 2 dB above the -20 dB level.

These results show very satisfactory agreement between the measured and predicted patterns and close alignment with the desired beam scanning. Based on these results, it is believed that the array is performing in a manner consistent with utility in a communications application.

VI. CONCLUDING REMARKS

A seven element S-band phased array based on the coupled oscillator beam steering concept has been fabricated. We have described an experimental investigation of the behavior of this array in which several theoretically predicted characteristics of such an array have been verified experimentally. While some difficulty was encountered initially, ultimately, the array provided an agile beam which could be steered from boresight to nearly 13 degrees by merely adjusting the voltages applied to the tuning ports of the end VCOs in the array. High efficiency, however, will require additional attention to the impedance match between the oscillator outputs and the radiating elements; a match which was not optimal in the present experiment due to the difference between the design frequency of the patch elements and the ultimate ensemble frequency of the array.

ACKNOWLEDGMENTS

The research described in this paper was performed by the Center for Space Microelectronics Technology, Jet Propulsion Laboratory, California Institute of Technology, and was sponsored by the Ballistic Missile Defense Organization through an agreement with the National Aeronautics and Space Administration.

REFERENCES

1. P. Liao and R. A. York, "A New Phase Shifterless Beam-Scanning Technique Using Arrays of Coupled Oscillators," *IEEE Trans. Microwave Theory and Tech.*, MTT-41, pp. 1810-1815, October 1993.
2. R. A. York, "Nonlinear Analysis of Phase Relationships in Quasi-Optical Oscillator Arrays," *IEEE Trans. Microwave Theory and Tech.*, MTT-41, pp. 1799-1809, October 1993.
3. H.-C. Chang, E. S. Shapiro, and R. A. York, "Influence of the Oscillator Equivalent Circuit on the Stable Modes of Parallel-Coupled Oscillators," *IEEE Trans. Microwave Theory and Tech.*, MTT-45, pp. 1232-1239, August 1997.
4. R. Adler, "A Study of Locking Phenomena in Oscillators," *Proc. IEEE*, 61, pp. 1380-1385, October 1973.
5. R. J. Pogorzelski, P. F. Maccarini, and R. A. York, "A Continuum Model of the Dynamics of Coupled Oscillator Arrays for Phase Shifterless Beam-Scanning," *IEEE Trans. Microwave Theory and Tech.*, MTT-47, April 1999.
6. R. A. York, P. Liao, and J. Lynch, "Oscillator Array Dynamics with Broadband N-Port Coupling Networks," *IEEE Trans. Microwave Theory and Tech.*, MTT-42, pp. 2040-2045, November 1994.
7. K. D. Stephan, "Inter-Injection-Locked Oscillators for Power Combining and Phased Arrays," *IEEE Trans. Microwave Theory and Tech.*, MTT-34, pp. 1017-1025, October 1986.

Figure Captions

Figure 1. MMIC-based voltage controlled oscillator layout.

Figure 2. Three oscillator array.

Figure 3. Closeup of one oscillator of the three oscillator array.

Figure 4. The seven element oscillator array.

Figure 5. Closeup of one oscillator of the seven element array.

Figure 6. Partial schematic of the seven oscillator array.

Figure 7. Partial layout of the seven oscillator array.

Figure 8. Tuning curves of the uncoupled oscillators.

Figure 9. Tuning curves of the coupled oscillators.

Figure 10. Configuration of a single S-band microstrip patch radiator.

Figure 11. Calculated performance of the single S-band patch radiator.

Figure 12. Calculated radiation patterns of the seven element S-band microstrip array.

Figure 13. The seven element phased array antenna.

Figure 14. Measured return loss of one patch element of the seven element array.

Figure 15. Measured array pattern of the seven element array with the oscillator circuit replaced with a master oscillator and a seven way power divider.

Figure 16. Range measurement setup.

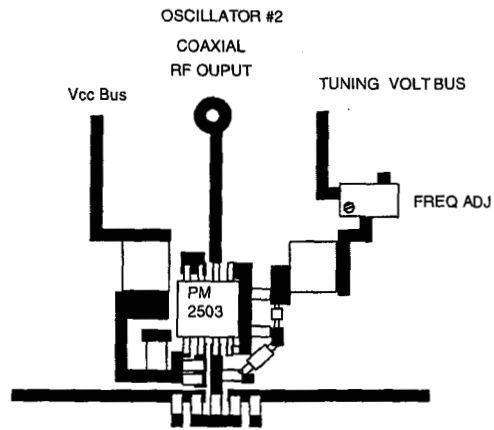
Figure 17. Experimental array pattern for zero degree scan.

Figure 18. Experimental array pattern for 6.38 degree scan.

Figure 19. Experimental array pattern for 9.59 degree scan.

Figure 20. Experimental array pattern for 12.84 degree scan.

Figure 21. Comparison of patterns at 0 and 180 degrees of roll and 6.38 degree scan.



Circuit Layout (typical)

Figure 1. MMIC-based voltage controlled oscillator layout.

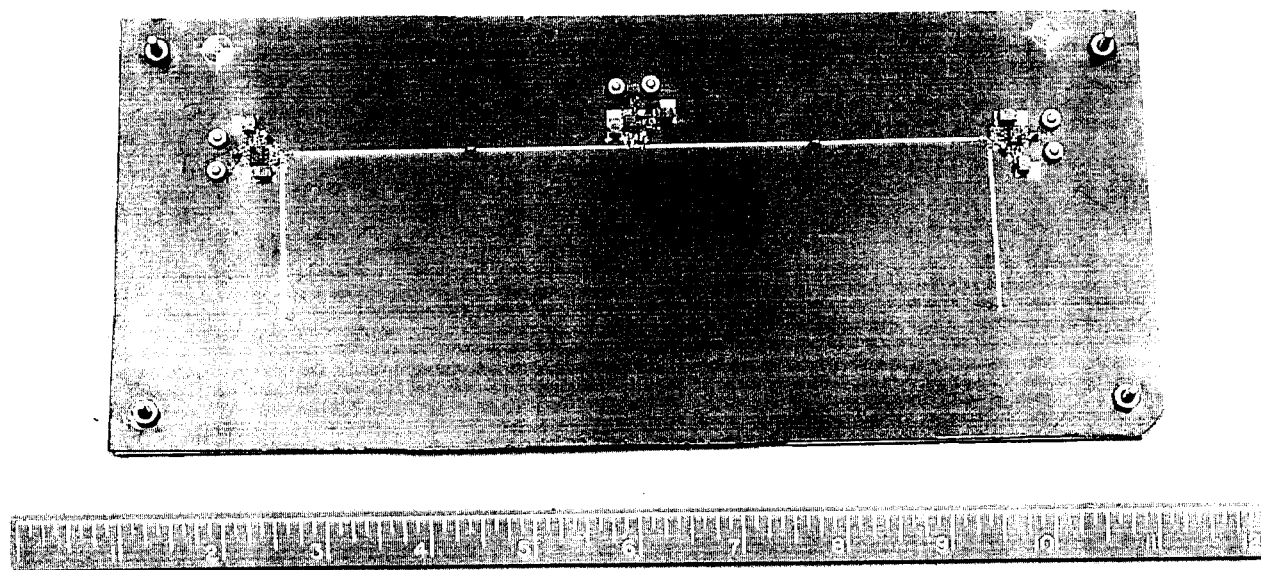


Figure 2. Three Oscillator Array.

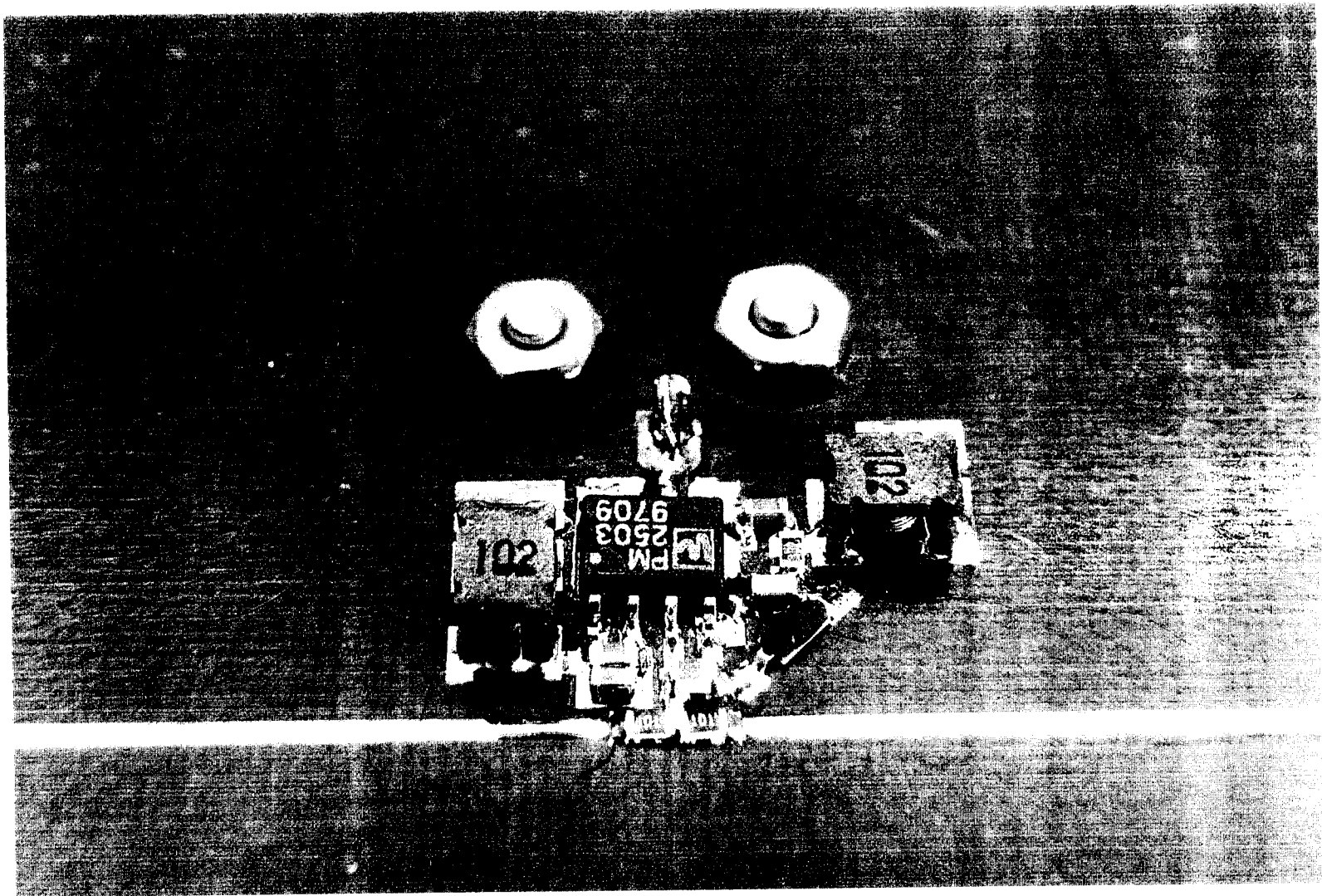


Figure 3. Closeup of the Center Oscillator
of the Three Oscillator Array.

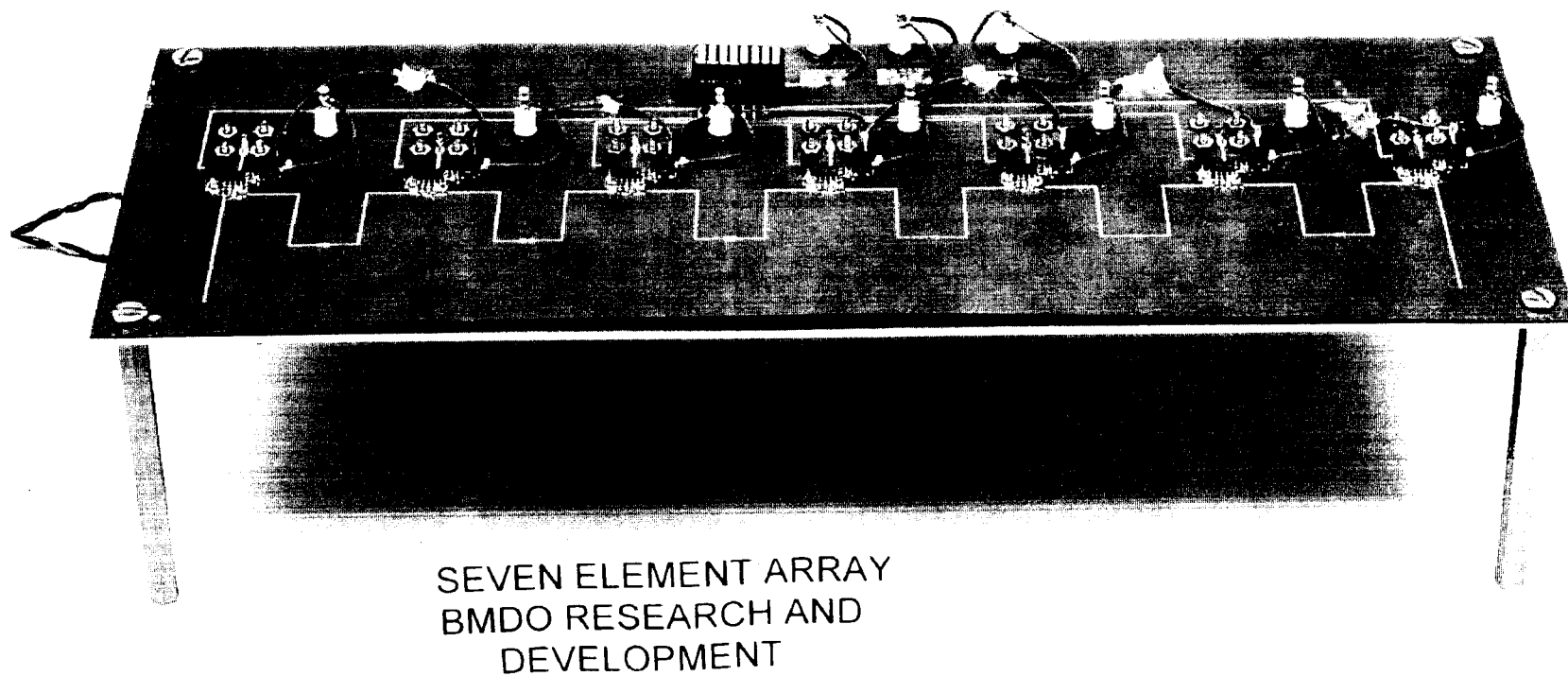


Figure 4. Seven Element Experimental Test Board.

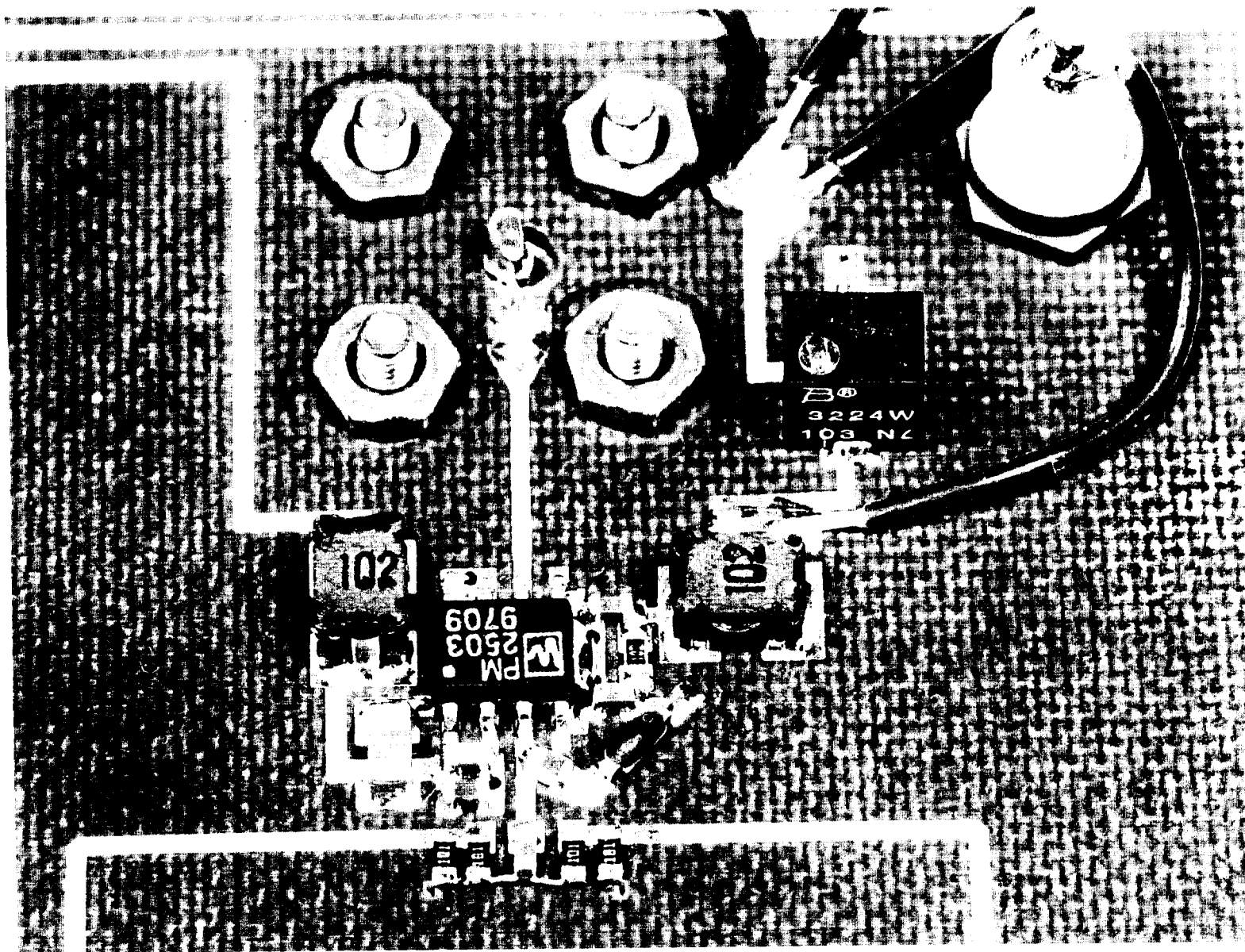


Figure 5. Close up of Center Oscillator Circuit of Figure 4.

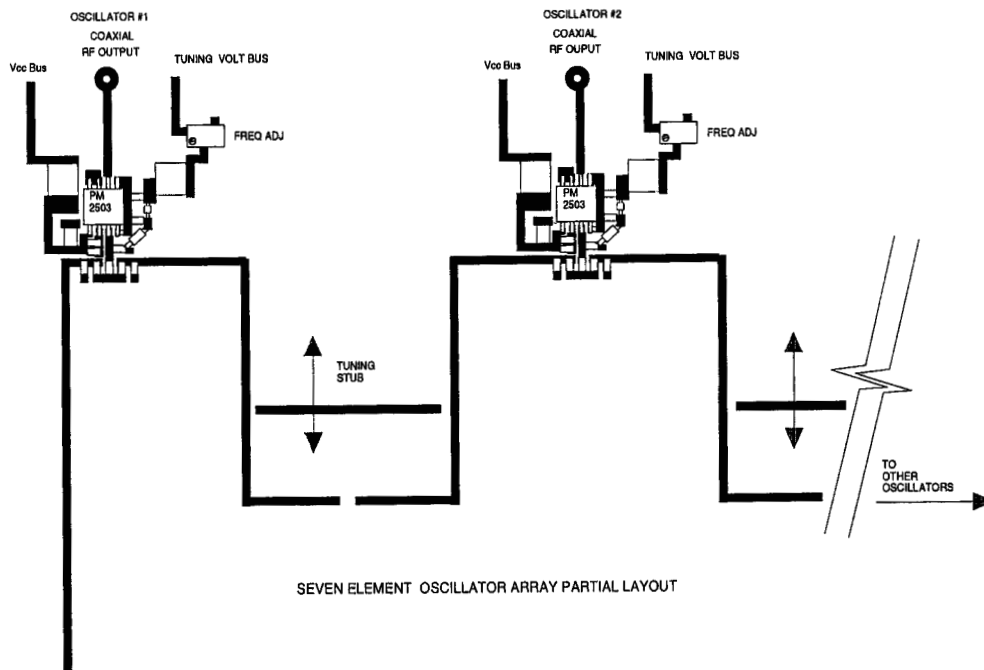


Figure 7. Circuit board layout.

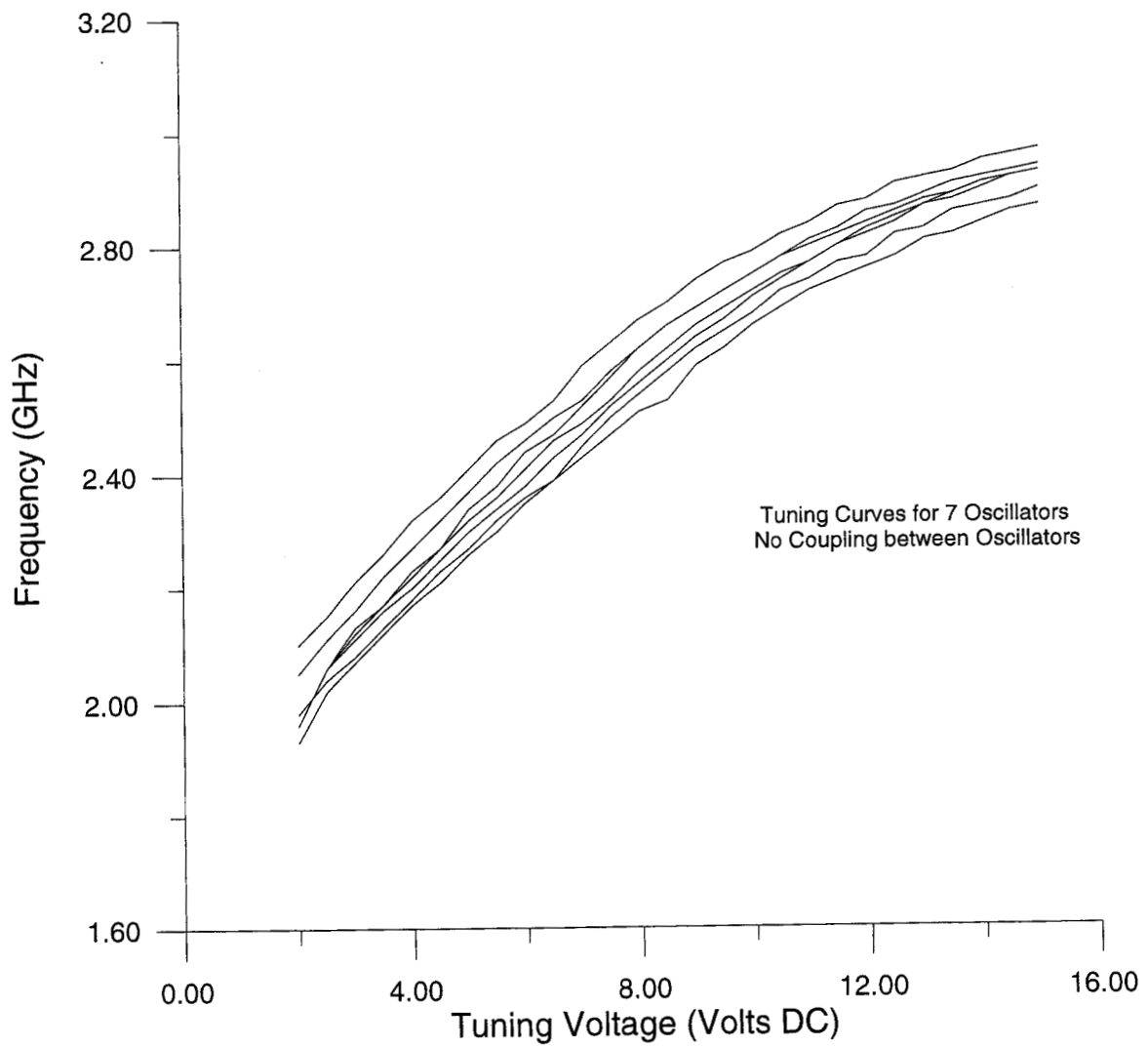


Figure 8. Oscillator tuning curves.

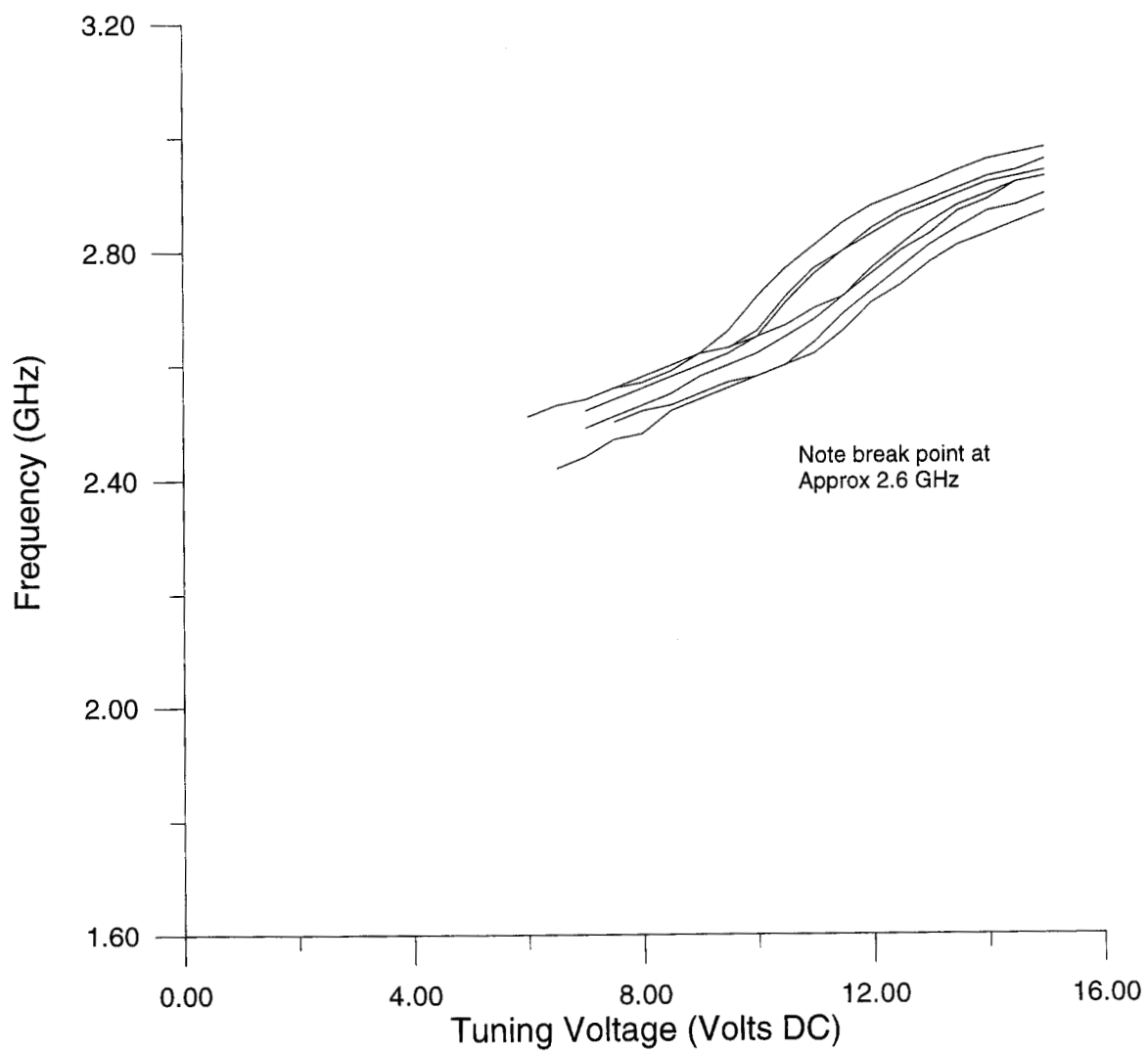


Figure 9. Coupled oscillator tuning curves.

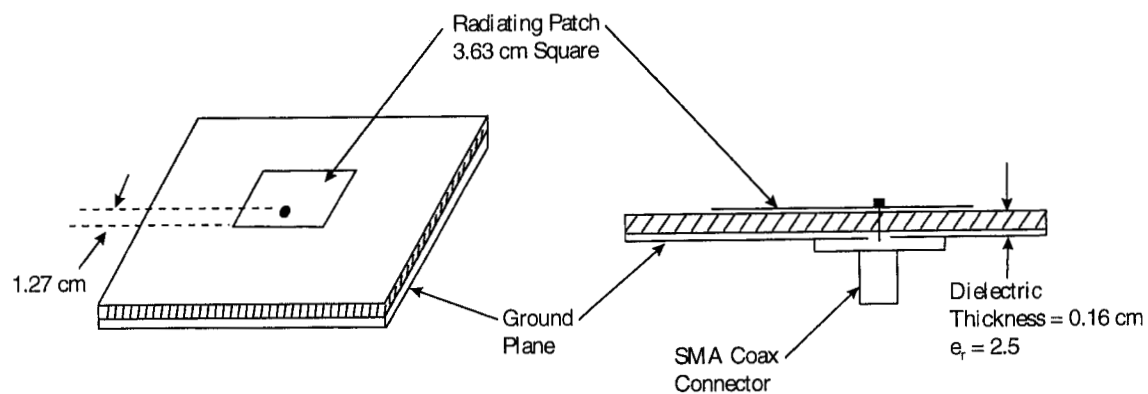


Figure 10. Configuration of a single S-band microstrip patch radiator

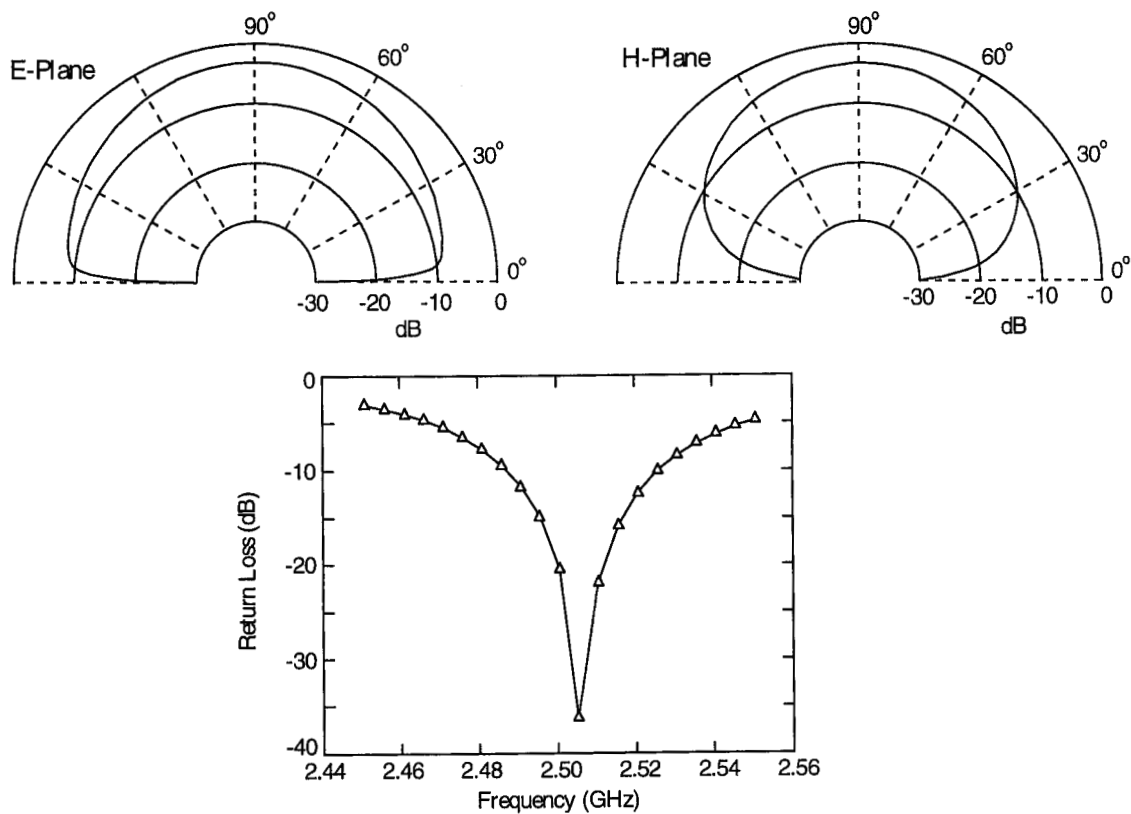


Figure 11. Calculated performance of the single S-band patch radiator

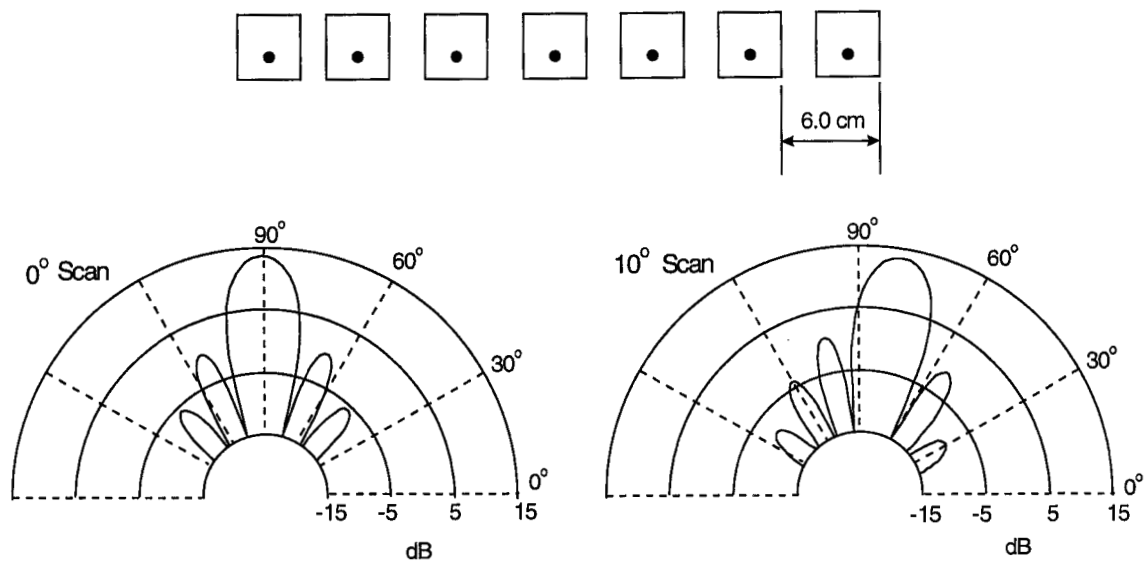
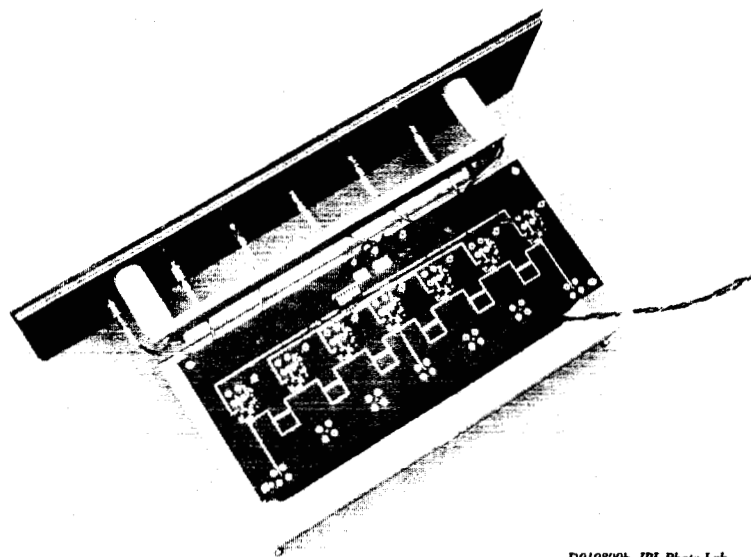
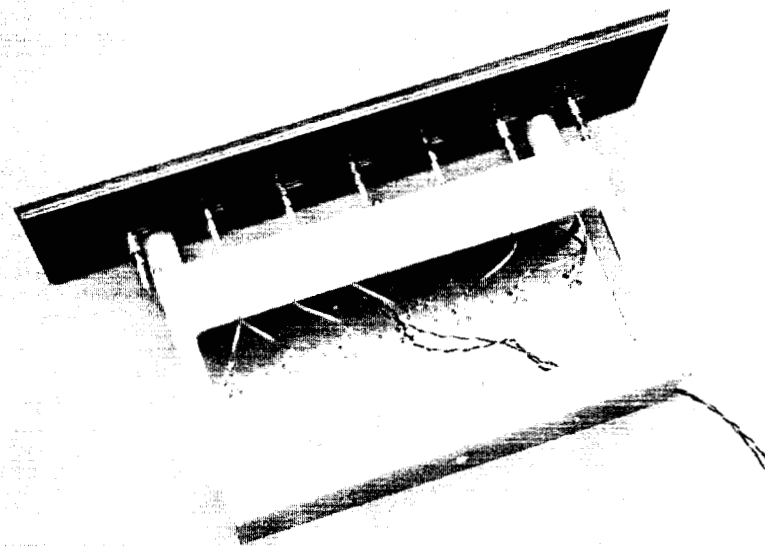


Figure12. Calculated radiation patterns of the seven element S-band microstrip array



D010899b JPL Photo Lab



D010899a JPL Photo Lab

Figure 13. The Seven Element Phased Array Antenna.

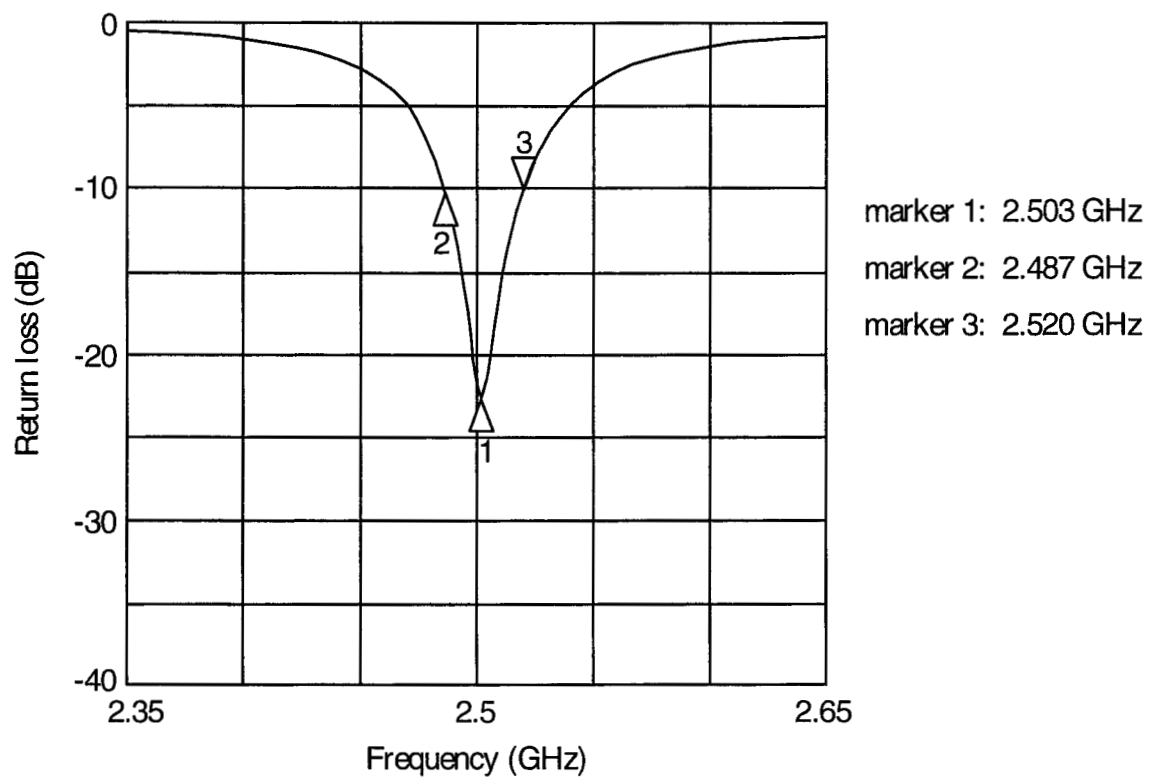


Figure14. Measured return loss of one patch element of the seven element array.

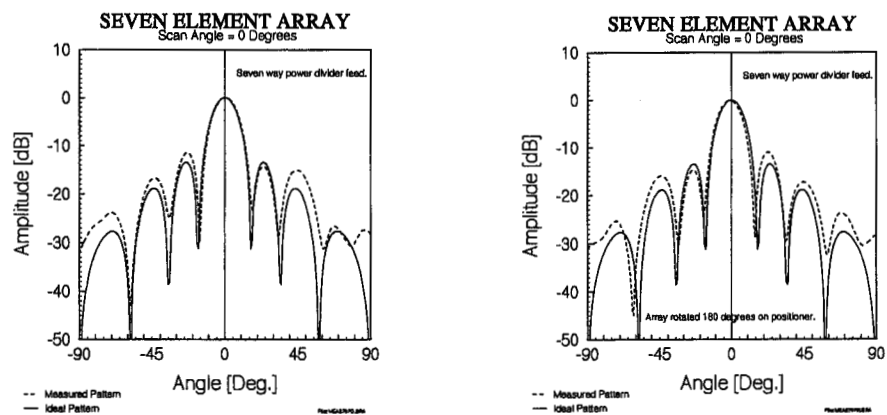


Figure 15. Measured array pattern of the seven element array with the oscillator circuit replaced with a master oscillator and a seven way power divider.

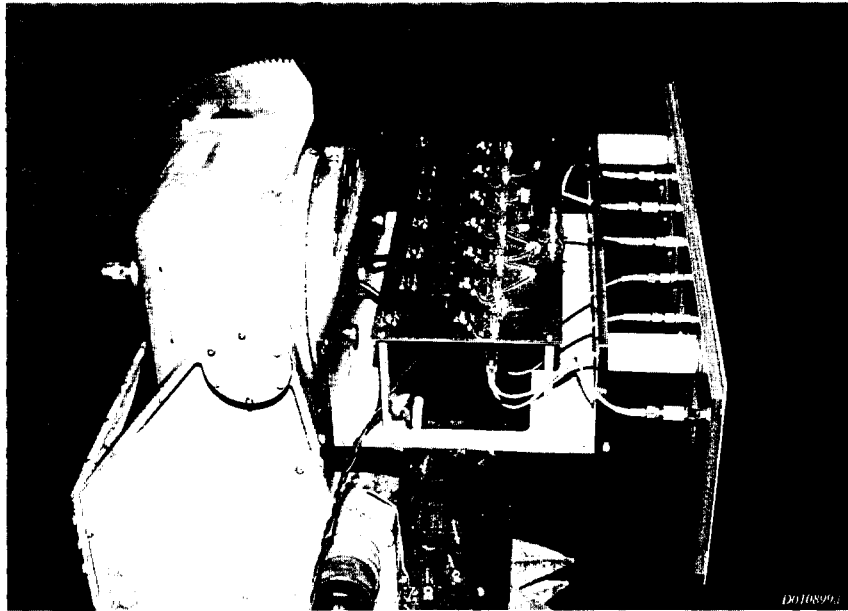
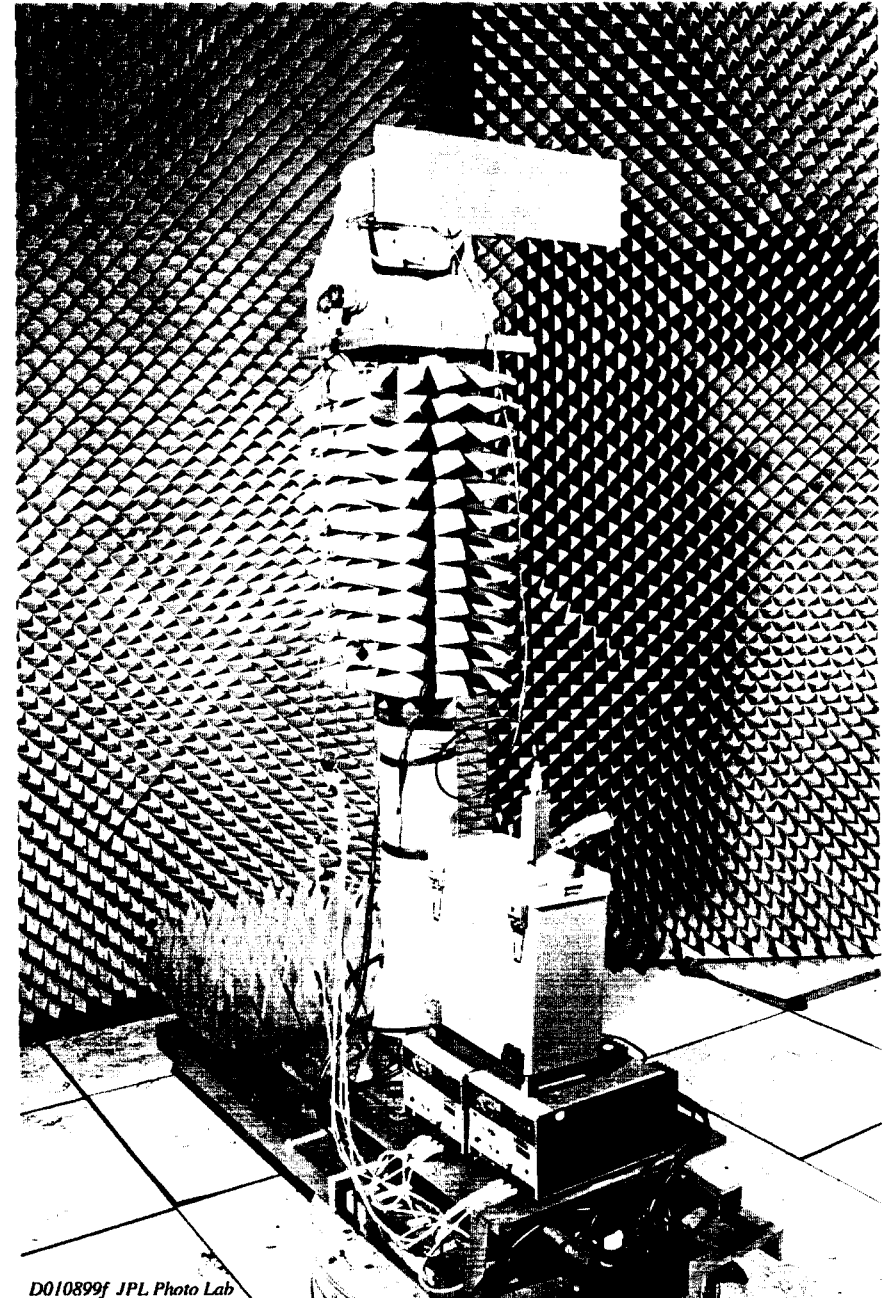
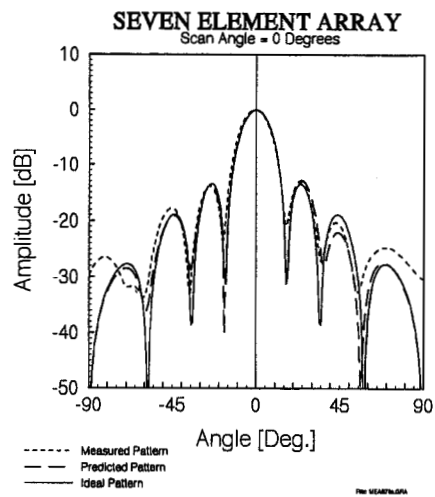


Figure 16. Seven Element Array on Range Positioner.

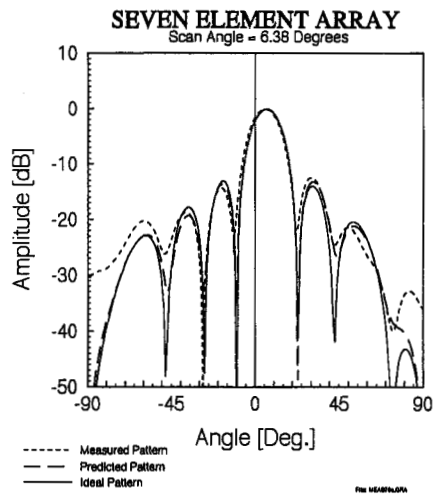


D010899f JPL Photo Lab



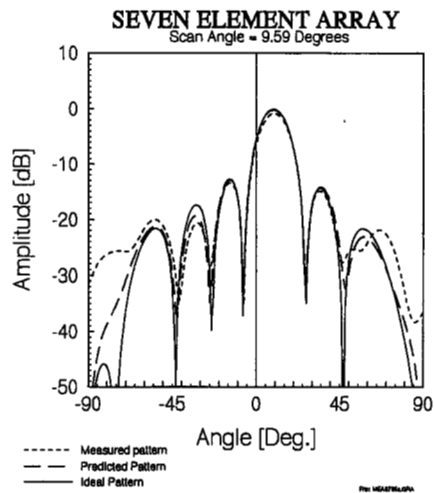
Osc.	Freq. (GHz)	Pwr (dBm)	Tuning Voltage	Phase (Deg.)
1	2.530	- 9.67	7.39	0.0
2	2.530	- 9.50	8.40	-4.9
3	2.530	- 9.17	9.65	-6.7
4	2.546	-10.00	6.99	6.8
5	2.530	- 9.17	8.01	0.0
6	2.530	- 8.83	8.29	-5.6
7	2.530	-10.83	8.72	2.3

Figure17. Experimental array pattern for zero degree scan.



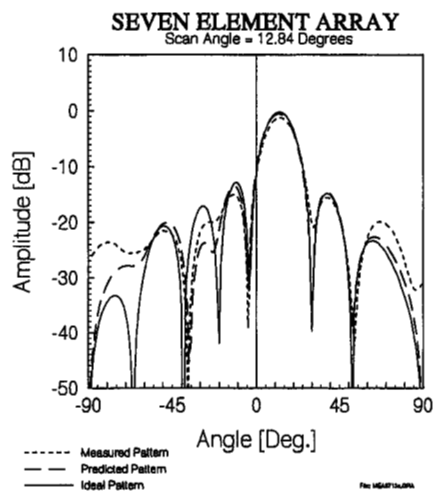
Osc.	Freq. (GHz)	Pwr (dBm)	Tuning Voltage	Phase (Deg.)
1	2.547	- 9.00	7.89	0.0
2	2.530	- 9.67	8.40	- 32.2
3	2.530	- 9.50	9.65	- 45.5
4	2.546	-10.00	6.99	- 59.6
5	2.530	- 9.17	8.01	- 83.6
6	2.530	- 9.00	8.29	-106.5
7	2.519	- 10.83	8.50	-121.7

Figure 18. Experimental array pattern for 6.38 degree scan



Osc.	Freq. (GHz)	Pwr (dBm)	Tuning Voltage	Phase (Deg.)
1	2.553	- 8.83	8.03	0.0
2	2.530	- 9.67	8.40	- 37.0
3	2.530	- 9.50	9.65	- 63.4
4	2.546	-10.17	6.99	- 99.7
5	2.530	- 9.17	8.01	-123.5
6	2.530	- 9.17	8.29	-155.0
7	2.514	-11.17	8.37	-179.5

Figure19. Experimental array pattern for 9.59 degree scan.
[Note that the normalization for this measurement was obtained from
a second measurement carried out one day later.]



Osc.	Freq. (GHz)	Pwr (dBm)	Tuning Voltage	Phase (Deg.)
1	2.554	-8.83	8.07	0.0
2	2.530	-9.67	8.40	- 49.4
3	2.530	-9.50	9.65	- 71.6
4	2.546	-10.33	6.99	-128.0
5	2.530	-9.17	8.01	-156.0
6	2.530	-9.50	8.29	-192.0
7	2.496	-12.50	7.95	-242.0

Figure 20. Experimental array pattern for 12.84 degree scan.

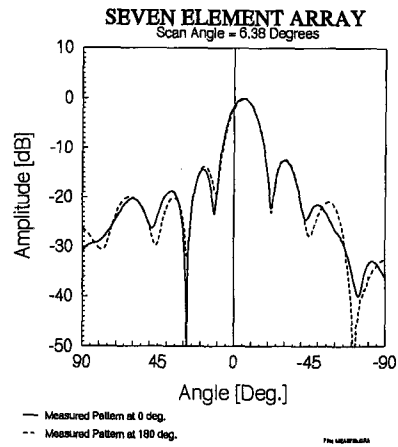


Figure 21. Comparison of patterns at 0 and 180 degrees of roll and 6.38 degree scan.